

Computation and Communication Efficient Federated Unlearning via On-server Gradient Conflict Mitigation and Expression

Minh-Duong Nguyen¹, Senura Hansaja², Le-Tuan Nguyen¹, Quoc-Viet Pham³,
Ken-Tye Yong², Nguyen H. Tran², Dung D. Le¹

¹ VinUniversity, ² University of Sydney, ³ Trinity College Dublin

{duong.nm2, tuan.nl, dung.ld}@vinuni.edu.vn, viet.pham@tcd.ie

{senu.wanasekara, nguyen.tran, ken.yong}@sydney.edu.au

Abstract

Federated Unlearning (FUL) aims to remove specific participants' data contributions from a trained Federated Learning model, thereby ensuring data privacy and compliance with regulatory requirements. Despite its potential, progress in FUL has been limited due to several challenges, including the cross-client knowledge inaccessibility and high computational and communication costs. To overcome these challenges, we propose Federated On-server Unlearning (FOUL), a novel framework that comprises two key stages. The learning-to-unlearn stage serves as a preparatory learning phase, during which the model identifies and encodes the key features associated with the forget clients. This stage is communication-efficient and establishes the basis for the subsequent unlearning process. Subsequently, on-server knowledge aggregation phase aims to perform the unlearning process at the server without requiring access to client data, thereby preserving both efficiency and privacy. We introduce a new data setting for FUL, which enables a more transparent and rigorous evaluation of unlearning. To highlight the effectiveness of our approach, we propose a novel evaluation metric termed time-to-forget, which measures how quickly the model achieves optimal unlearning performance. Extensive experiments conducted on three datasets under various unlearning scenarios demonstrate that FOUL outperforms the Retraining in FUL. Moreover, FOUL achieves competitive or superior results with significantly reduced time-to-forget, while maintaining low communication and computation costs. Reproducible code is available [here](#).

1. Introduction

Federated Learning (FL) has enabled the collaborative training of machine learning models across decentralized data sources or clients, facilitating the development of more

accurate and robust models. Local clients benefit by getting an aggregated and more powerful personalized model without sharing their private data. With the recent introduction of data protection laws such as the General Data Protection Regulation (GDPR) [34] in the European Union, it has become essential to provide clients with the right to erasure regarding their own private data, even if that data has already been used to train the global model in federated learning. Federated Unlearning (FUL) [38] aims to address this challenge by developing methods for removing specific information from globally trained models. FUL plays a critical role in supporting the *right to be forgotten* paradigm, wherein the removal of a client's data from the model may be legally or ethically mandated.

In the field of FUL, two primary categories of methods have emerged: retraining-based methods [20], approximate unlearning methods [4, 43] (see Appendix A for more details). Retraining-based methods involve retraining the entire FL system from scratch using a dataset that excludes the forget set, thereby ensuring that the final model no longer reflects the influence of the data to be forgotten. While these methods often achieve state-of-the-art unlearning performance, retraining approaches are computationally intensive. Consequently, such approaches are impractical and unscalable for real-world FL applications due to substantial computational and communication overhead.

To mitigate the computational burden of retraining-based unlearning, recent studies have shifted toward approximate unlearning methods [4, 43, 46]. These approaches typically focus on local unlearning or selective client aggregation, which are particularly effective in federated feature unlearning settings, where both the retain and forget subsets are available at the client side. In such cases, unlearning can be performed locally on clients and the updated models are aggregated in the same manner as vanilla FL [11].

However, when the objective shifts to client-wise unlearning, where the goal is to erase the entire contribu-

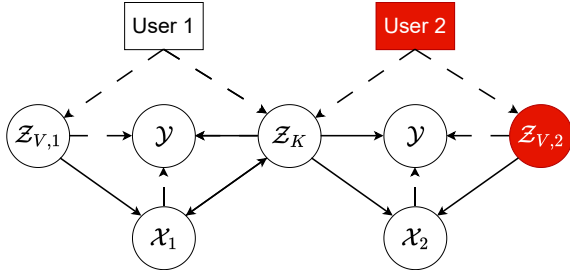


Figure 1. Extension of the causal structure model to the multi-client setting. Following [28], the causal factors Z_K represent the domain-invariant characteristics. Consequently, when unlearning a client, removing Z_K may reduce the amount of useful information necessary for predicting \mathcal{Y} . In contrast, unlearning the non-causal factors $Z_{V,2}$ primarily removes domain-specific information from client 2, while having a smaller impact on the information relevant to the classification of \mathcal{Y} . Dashed lines denote edges that may vary across clients or be absent in certain scenarios, solid lines indicate edges that remain invariant across all clients.

tion of specific clients, the problem becomes substantially more challenging. The primary difficulty arises because the forget clients lack access to the retain dataset. To be more specific, current unlearning formulations are typically feasible only when both retain and forget data are available, as the unlearning objective is often expressed as $\mathcal{L}_{\text{unlearn}} = \mathcal{L}_{\text{retain}}(\theta; \mathcal{D}_r) - \mathcal{L}_{\text{forget}}(\theta; \mathcal{D}_f)$. Consequently, existing client-wise FUL methods rely solely on the retain set \mathcal{D}_r , while ignoring the forgotten set \mathcal{D}_f . In this work, we propose Federated On-server UnLearning (FOUL), a novel algorithm designed for client-wise FUL that efficiently and faithfully removes targeted knowledge without compromising the knowledge of retain clients. FOUL achieves this while significantly reducing the computational overhead of the unlearning process. ❶ To mitigate the high cost of unlearning, we introduce the principle of learning to unlearn (L2U) during the learning stage. Specifically, FOUL disentangles the feature extractor into two sub-networks: a causal featurizer, which captures domain-invariant representations, and a non-causal featurizer, which encodes domain-specific information. We demonstrate that unlearning only the non-causal features effectively removes domain-specific (i.e., forget-set-related) knowledge while preserving generalizable, domain-invariant information crucial to the retain set (see Fig. 1). ❷ To enable the joint utilization of knowledge from both retain and forget client sets, FOUL enforces aggregated gradients to remain aligned with the retain clients while intentionally conflicting with the forget clients, ensuring effective unlearning. Unlike prior methods such as [49], FOUL requires no on-server data access, thereby preserving both communication efficiency and data privacy under the FL paradigm. Our key contributions are summarized as follows:

1. We propose FOUL, an efficient FUL algorithm which consists of two stages, L2U via model disentanglement, and on-server unlearning performed on the domain-specific disentangled model via gradient matching.
2. We introduce an approach for leveraging domain generalization datasets (e.g., PACS, VLCS, OfficeHome) to benchmark FUL performance. Additionally, we propose a new metric, time-to-forget, which quantifies how quickly a model achieves optimal unlearning.
3. We experimentally demonstrate the effectiveness of the proposed method across various client-wise unlearning settings, comparing it against 9 FUL methods.

2. Preliminaries

Notations: We abuse $|\cdot|$ as a number of elements in the subset, \perp as independent relationship between two subsets. Suppose that there is a user set \mathcal{U} . Let $\mathcal{D} = \{(x_i, y_i)\}_{i=1}^{|\mathcal{D}|}$, where x_i and y_i represent the input and its corresponding output, respectively. In our work, we refer Z_K, Z_V as the causal and non-causal representation set, respectively. Due to the mini-batch learning, we abuse $Z_K = \{z_K^{(i)} | i \in B\}$ as the causal representation set within the batch with size B . The non-causal representation set Z_V applies the same rule.

2.1. Federated Unlearning

Definition 1 (Forget user set) Given a training user set \mathcal{U} , the forget user set is a subset of \mathcal{U} whose data is intended to be removed or unlearned, denoted by \mathcal{U}_F .

Definition 2 (Retain user set) A retain user set is the set of users which required to be memorized in the FL system, denoted as \mathcal{U}_R , including all other data that is not targeted for removal and is crucial for maintaining the general knowledge and functionality of the model, i.e., $\mathcal{U}_R = \mathcal{U} \setminus \mathcal{U}_F$.

Given the two above definitions, FUL consists of two primary processes: 1) learning stage, and 2) unlearning stage.

Definition 3 (Learning Stage) The goal of learning stage is to collaboratively learn a machine learning model θ over the dataset $\mathcal{D} \triangleq \bigcup_{u \in \mathcal{U}} \mathcal{D}_u$:

$$\theta_{\text{learn}}^* = \arg \min_{\theta} \frac{1}{|\mathcal{U}|} \sum_{u \in \mathcal{U}} \mathcal{L}(\theta; \mathcal{D}_u), \quad (1)$$

where $\mathcal{L}(\theta; \mathcal{D}_u) = \mathbb{E}_{(x,y) \sim \mathcal{D}_u} [\ell(\theta; (x,y))]$ is the empirical loss of user u , and during learning stage, each user minimizes their empirical risk $\mathcal{L}(\theta; \mathcal{D}_u)$, θ_{learn}^* is the final model trained by the learning stage.

The unlearning stage is conducted following the learning stage, with the objective of obtaining an unlearned FL model, denoted as θ_{unlearn} .

Definition 4 (Unlearning Stage) *The goal of the unlearning stage is to achieve performance comparable to a model trained exclusively on the remaining dataset, while ensuring that knowledge about the forget dataset is forgotten.*

$$\theta_{unlearn}^* = \arg \max_{\theta} \frac{1}{|\mathcal{U}_{\mathcal{F}}|} \sum_{v \in \mathcal{U}_{\mathcal{F}}} \mathcal{L}(\theta; \mathcal{D}_v), \quad (2)$$

$$s.t. \frac{1}{|\mathcal{U}_{\mathcal{R}}|} \sum_{u \in \mathcal{U}_{\mathcal{R}}} \left[\mathcal{L}(\theta_{unlearn}^*; \mathcal{D}_u) - \mathcal{L}(\theta_{learn}^*; \mathcal{D}_u) \right] \leq \delta,$$

where we solve 2 by initializing θ as θ_{learn} before using standard iterative optimization technique. $\theta_{unlearn}^*$ is the target unlearned model, and θ_{learn}^* is the pre-trained model of θ defined during the learning stage. δ is an arbitrarily small threshold which constraint the knowledge divergence between $\theta_{unlearn}^*$ and θ_{learn}^* for remaining set.

3. Methods

In this section, we present the FOUL algorithm, which operates through a two-stage unlearning process: (1) Learning to unlearn, where the model is prepared during the initial learning stage to facilitate efficient future unlearning, and (2) On-server gradient matching, where unlearning is executed by manipulating gradients directly on the server.

3.1. Learning to unlearn

Existing FUL approaches predominantly focus on retraining or adjusting the model from scratch [11]. However, this strategy incurs substantial computational overhead on individual clients and increases communication costs due to frequent model transmission between clients and the server. In practice, not all model parameters are equally influenced by the data that must be forgotten [20, 56]. Many components of the model capture domain-invariant knowledge that remains relevant to both the retained and forgotten data, and therefore do not require modification during the unlearning process. To this extent, recent studies attempt to identify and unlearn only a subnetwork of the model by analyzing gradient conflicts [20, 56]. However, because the model changes across unlearning rounds, the subnetwork identification must be repeatedly performed, leading to significant additional computation overhead. To address this limitation, we propose L2U, which disentangles the model into domain-invariant and domain-specific subnetworks during training. By isolating only the domain-specific component for unlearning, L2U preserves model stability across unlearning rounds while reducing computation and communication overhead.

3.1.1 Motivation

The core idea of L2U via disentanglement is to learn disentangled representations by imposing invariance constraints

on two spaces \mathcal{Z}_K and \mathcal{Z}_V . Our design is inspired by the causal-structural representation learning [29], which is defined as follows:

Definition 5 (Causal Structured Model [29]) *The data \mathcal{X} composes of two distinct representations, i.e., causal factors \mathcal{Z}_K and non-causal factors \mathcal{Z}_V , and unexplained noise variables $\mathcal{V}_1, \mathcal{V}_2$ that are jointly independent, i.e., $\mathcal{Z}_K \perp\!\!\!\perp \mathcal{Z}_V \perp\!\!\!\perp \mathcal{V}_1 \perp\!\!\!\perp \mathcal{V}_2$.*

- *The causal factors \mathcal{Z}_K should be separated from the non-causal factors \mathcal{Z}_V , i.e., $\mathcal{Z}_K \perp\!\!\!\perp \mathcal{Z}_V$. Thus, performing an intervention upon \mathcal{Z}_V does not make changes to \mathcal{Z}_K .*
 - *The combination of causal and non-causal factors $\mathcal{Z}_K, \mathcal{Z}_V$ should be sufficient to the data \mathcal{X} reconstruction task, i.e., $\mathcal{X} \triangleq f(\mathcal{Z}_K, \mathcal{Z}_V, \mathcal{V}_1)$.*
 - *The causal factors \mathcal{Z}_K should be causally sufficient for the classification task $\mathcal{X} \rightarrow \mathcal{Y}$, i.e., $\mathcal{Y} \triangleq h(\mathcal{Z}_K, \mathcal{V}_2)$.*
- Here, f, h can be regarded as unknown structural functions.

Given that the noise variables are unexplainable, we restrict our focus to the causal and non-causal representations. To relate these representations to data features across different domains, we adopt the following definition.

Definition 6 (Causal and non-causal representations [29])

Causal factors \mathcal{Z}_K have a direct causal influence on both X and Y , making them domain-invariant. In contrast, \mathcal{Z}_V represents non-causal factors that only causally affect X and typically contain domain-specific information.

Definition 5 formalizes the feasibility of disentangling the model into two independent factors. The causal invariance theorem provides the theoretical foundation for our unlearning objective. In the unlearning process, our goal is to remove the knowledge associated with the forget client set while preserving that of the retain client set. Therefore, unlearning can be viewed as reducing the information encoded in the non-causal (domain-specific) representations, since modifying the causal representations would inevitably impair the retained knowledge.

Definition 7 (Causal Principle in Unlearning)

To preserve the knowledge of the retain set while removing that of the forget set, the main objective of unlearning is to reduce the information encoded by the non-causal featurizer.

Motivated by this principle, L2U disentangles the feature extractor into a causal featurizer θ_K and a non-causal featurizer θ_V . During the subsequent unlearning phase, updates are applied exclusively to the non-causal featurizer, while the causal featurizer remains frozen. This strategy enables FOUL to efficiently remove domain-specific knowledge from the forget set without compromising the generalizable representations learned from the retain set.

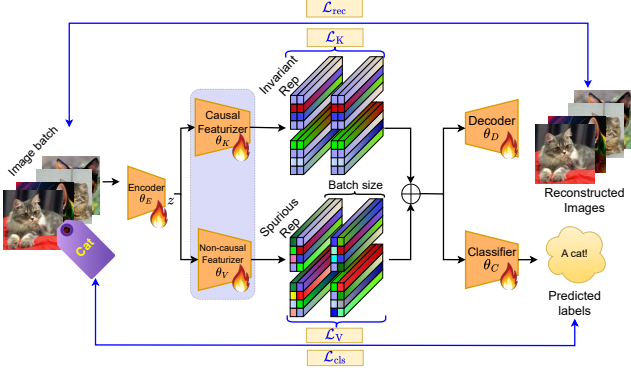


Figure 2. The learning on a single local client in the L2U stage. Featurizers are trained to disentangle knowledge into invariant and variant representations.

3.1.2 Learning for Representation Featurizer

General learning framework. To achieve effective disentanglement learning in L2U, it is essential that the learned representations exhibit both causal and non-causal characteristics. These two components must not only capture distinct aspects of the data but also jointly contribute to form meaningful and interpretable representations. Moreover, the causal representations are required to preserve the underlying causal structure that remains invariant across domains.

Overall, the central idea is to impose representation disentanglement within the model, where two distinct latent components are learned: causal representations, which are invariant and informative for classification, and non-causal representations, which capture variant information sensitive to data perturbations. Together, these two representations contribute to accurate data reconstruction. Based on this formulation, the proposed L2U stage is expressed as a bi-level optimization problem:

$$\min_{\theta} \left[\mathcal{L}_{L2U}(\theta) = \frac{1}{U} \sum_{u=1}^U \mathcal{L}_{L2U}(\theta_u) \right], \quad (3)$$

$$\text{s.t. } \mathcal{L}_{L2U}(\theta_u) = \min_{\theta_u} [\alpha_V \mathcal{L}_V + \alpha_K \mathcal{L}_K + \alpha_{gtc} \mathcal{L}_{gtc} + \mathcal{L}_{rec}],$$

where \mathcal{L}_V , \mathcal{L}_K , \mathcal{L}_{gtc} , and \mathcal{L}_{rec} denote the non-causal, causal, ground truth classification, and reconstruction losses, respectively.

To facilitate the optimization of \mathcal{L}_{gtc} and \mathcal{L}_{rec} , auxiliary decoders (θ_2) and classifiers (ξ) are introduced. Each local model is parameterized as $\theta_u = \{\theta_{E,u}, \theta_{K,u}, \theta_{V,u}, \theta_{D,u}, \theta_{C,u}\}$, where $\theta_{E,u}$ represents the shallow feature extractor; $\theta_{K,u}$ and $\theta_{V,u}$ are the causal and non-causal encoders, respectively; $\theta_{D,u}$ is the decoder; and $\theta_{C,u}$ is the classifier of client u .

The detailed two-stage optimization procedure for L2U

is presented in Appendix B, and the overall structure of the local model is depicted in Fig. 2.

Training Causal Featurizer. The goal of the causal featurizer is to extract class-discriminative features that are invariant to domain-specific, non-causal variations. To enforce this invariance, we train the model to generate highly compact representations for all samples belonging to the same class. By minimizing this intra-class distance, the model is encouraged to ignore superficial differences and focus on the essential, shared characteristics. The prototypical network framework [37] is exceptionally well-suited for this objective, as it explicitly learns a central prototype for each class. To achieve this, we train the causal performer using the prototypical network framework in the following manner:

$$\mathcal{L}_K = - \sum_{c=1}^C \log \frac{\exp(s(f_{\phi}(x), p_c))}{\sum_{i=1}^C \mathbb{1}_{[i \neq c]} \exp(s(f_{\phi}(x), p_i))}, \quad (4)$$

where $s(f_{\phi}(x), p_c)$ represents the cosine similarity between the encoded representations $f_{\phi}(x)$ and the approximated class prototype p_c . To approximate the prototype within the batch, we compute as [37] as $p_c = \frac{1}{|S_c|} \sum_{s_i, y_i \in S_c} f_{\phi}(x_i)$. $B_c \in B$ is the batch of data belonging to label c .

Training Non-causal Featurizer. To extract non-causal representations effectively, we maximize the empirical distance among representations within a specific label. However, two problems may arise during the maximization of the MSE between samples: **Ⓐ** When the MSE value is at its initial value (where the variance is relatively low, i.e., nearly 0), the optimization process prioritizes tasks with high initial losses. This prioritization can overshadow the learning of variant representations in the early stages. **Ⓑ** When the MSE value is already optimized, performing the maximization process further can increase the variance, potentially diminishing the learning of other tasks. To mitigate these problems, we adopt the hinge loss framework introduced in [2] in designing the variant loss \mathcal{L}_V :

$$\mathcal{L}_V = \frac{1}{C} \sum_{c=1}^C \max \left(0, 1 - \sqrt{\text{Var}(\mathcal{Z}_V^c) + \epsilon} \right), \quad (5)$$

where $\text{Var}(\mathcal{Z}_V^c)$ represents the variance among samples in the same class c , and

$$\text{Var}(\mathcal{Z}_V^c) = \mathbb{E}_{i \in B_c} \left[\left\| z_V^{(i)} - \mathbb{E}_{j \in B_c} \left(z_V^{(j)} \right) \right\|^2 \right]. \quad (6)$$

Incorporating the hinge loss brings the non-causal learning function into better alignment with other loss functions used in FOUL. This alignment involves initiating the optimization from higher values to mitigate trivial losses during the

initial phase, while setting a lower boundary at zero to prevent bias towards \mathcal{L}_V as the learning progresses.

Meaningful Representations. From Definition 5, the disentangled factors must be sufficient for the reconstruction task. Hence, our goal for training FOUL is twofold:

- The causal representations capture crucial information that accurately represents their respective label.
- The two extracted factors can be combined and collectively used to reconstruct the original data with the highest possible accuracy.

To achieve the first goal, it should be possible to predict a specific label from the causal factors \mathcal{Z}_K . We introduce the label classification function \mathcal{L}_{gtc} as follows:

$$\mathcal{L}_{\text{gtc}} = -\mathbb{E}_{i \in B} \left[P(y^{(i)}) \log P\left(f_{\xi}(z_K^{(i)})\right) \right], \quad (7)$$

where $f_{\xi} : \mathbb{R}^{d_{z_K}} \rightarrow \mathbb{R}$ is the classifier network, parameterized by ξ , handling the classification task for the causal factors $z_K^{(i)}$. $y^{(i)}$ is the label of data instance i . $P(\cdot)$ denotes the probability distributions.

To achieve the second goal, we employ the reconstruction loss \mathcal{L}_{rec} according to [22]. Specifically, we minimize the MSE between the original and its reconstructed data, while maximizing the KL divergence, and we enhance generalization by compelling the featurizer to output a distribution over the latent space instead of a single point. For instance,

$$\mathcal{L}_{\text{rec}} = \mathcal{L}_{\text{MSE}} - \mathcal{L}_{\text{KL}}. \quad (8)$$

3.2. Client-wise Unlearning

Besides the unlearning of only the non-causal featurizers, our objective is to propose an efficient strategy to aggregate knowledge from all participated users without the explosion of communication overheads. Therefore, the unlearned global model of the FL system may reduce the generalization gap with current centralized machine unlearning methods. The intuition behind our work is inherited from the invariant gradient direction of [21, 30, 36].

Assumption 1 (Invariant Gradient Direction [30])

Consider a model θ with task of finding domain-invariant features, the features generated by the model θ is domain-invariant if the two gradients $\nabla \mathcal{L}(\theta; \mathcal{D}_u)$, and $\nabla \mathcal{L}(\theta; \mathcal{D}_v)$, on different domains \mathcal{D}_u and \mathcal{D}_v point to a similar direction, i.e., $\langle \nabla \mathcal{L}(\theta; \mathcal{D}_u), \nabla \mathcal{L}(\theta; \mathcal{D}_v) \rangle > 0$.

Assumption 1 recommends a strategy for efficiently aggregating knowledge of distributed users for the FL system to achieve generalization. From Assumption 1, we can have the inverted assumption as follows:

Assumption 2 (Unlearning via Gradient Matching)

Considering a model θ with task of unlearning features, the features generated by the model θ suffers from negative transfer if the two gradients $\nabla \mathcal{L}(\theta; \mathcal{D}_u)$, and $\nabla \mathcal{L}(\theta; \mathcal{D}_v)$ does not point to a similar direction, i.e., $\langle \nabla \mathcal{L}(\theta; \mathcal{D}_u), \nabla \mathcal{L}(\theta; \mathcal{D}_v) \rangle < 0$.

Combining the two Assumptions 1 and 2, we come up with an idea to design an on-server unlearning approach based on gradient matching (see Fig. 3). Specifically, on the server, our target is to find an unlearning global gradient that satisfies Assumption 1 on the retain user set \mathcal{U}_R while satisfying Assumption 2 on the forget user set \mathcal{U}_F .

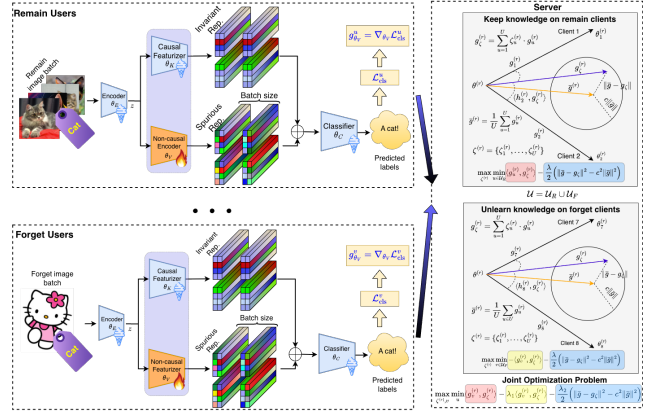


Figure 3. Unlearning stage with data-free on-server unlearning. Only the non-causal featurizer participates in this phase. The gradients of the non-causal featurizer from both retain and forget users are sent to the server for on-server gradient matching.

3.2.1 On-server gradient-based unlearning

Our target is to find an aggregated gradient so that it can make invariant directions towards gradients from the remaining clients \mathcal{U}_R , while making negative transfer towards gradients in forget clients \mathcal{U}_F . To reduce the computation cost of the optimization, we find the weights for the gradients aggregation so that it can form the optimal directions g_{FOUL} . For instance,

$$\theta_v^{(r)} = \theta_v^{(r-1)} - \eta g_{\text{FOUL}}, \quad (9a)$$

$$\text{s.t. } g_{\text{FOUL}} = \arg \max_g \left[\sum_{u \in \mathcal{U}_R} \langle g, \nabla(\phi_u^{(r)}; \mathcal{D}_u) \rangle - \sum_{v \in \mathcal{U}_F} \langle g, \nabla(\phi_v^{(r)}; \mathcal{D}_v) \rangle \right], \quad (9b)$$

$$\phi_u^{(r)} = \theta_g^{(r-1)} - \eta_l \nabla(\theta_g^{(r-1)}; \mathcal{D}_u), \forall u \in \mathcal{U}. \quad (9c)$$

By proposing Eq. (9), we establish the meta-objective function in Eq. (9a), which relies solely on client gradients as training signals. The optimization in Eq. (9b) aims to

maximize the cosine similarity between the aggregated gradient and the gradients of the retain clients, while minimizing the cosine similarity with the gradients of the forget clients. This mechanism enforces unlearning on the forget clients while preserving performance on the retain clients. However, one limitation of Eq. (9) is that the optimization over the model parameters g may exhibit poor generalization, since it operates without access to explicit training data at each optimization step. This issue becomes particularly severe for models with large parameter dimensionality. To mitigate this problem, we introduce a set of learnable weighting coefficients $\Gamma = \{\gamma_u^{(r)} \mid u \in \mathcal{U}, \sum_{u \in \mathcal{U}} \gamma_u^{(r)} = 1\}$, and reformulate the global gradient as $g = \sum_{u \in \mathcal{U}} \gamma_u^{(r)} \nabla \mathcal{L}(\phi(\phi_u^{(r)}; \mathcal{D}_u))$. This parameterization substantially reduces the optimization space: instead of learning the full parameter vector of dimension d , we now only optimize over U coefficients, where $U \ll d$. Based on this reformulation, we derive the following theorem.

Theorem 1 (FOUL solution) *Given $\Gamma = \{\gamma_u^{(r)} \mid u \in \mathcal{U}, \sum_{u \in \mathcal{U}} \gamma_u^{(r)} = 1\}$ is the set of learnable coefficients at each round r , where $\mathcal{U} = \{\mathcal{U}_{\mathcal{R}}, \mathcal{U}_{\mathcal{F}}\}$. Optimal unlearning gradient $\nabla_{FOUL}^{(r)}$ is characterized as follows:*

$$\nabla_{FOUL}^{(r)} = \nabla_{FL}^{(r)} + \frac{\kappa \|\nabla_{FL}^{(r)}\|}{\|\nabla_{\Gamma_{\mathcal{R}}}^{(r)} - \nabla_{\Gamma_{\mathcal{F}}}^{(r)}\|} (\nabla_{\Gamma_{\mathcal{R}}}^{(r)} - \nabla_{\Gamma_{\mathcal{F}}}^{(r)}), \quad (10)$$

$$\text{s.t. } \Gamma_{\mathcal{R}}^*, \Gamma_{\mathcal{F}}^* = \arg \min_{\Gamma_{\mathcal{R}}, \Gamma_{\mathcal{F}}} (\nabla_{\Gamma_{\mathcal{R}}}^{(r)} - \nabla_{\Gamma_{\mathcal{F}}}^{(r)}) \cdot \nabla_{FL}^{(r)} + \sqrt{\kappa} \|\nabla_{FL}^{(r)}\| \|\nabla_{\Gamma_{\mathcal{R}}}^{(r)} - \nabla_{\Gamma_{\mathcal{F}}}^{(r)}\|.$$

Theorem 1 gives us an on-server optimization approach via the gradient matching without the need for local data accessibility. The detailed algorithm of the unlearning stage of FOUL is detailed in Appendix D.

4. Experimental Setup

Unlearning Scenarios. To effectively simulate the client data unlearning process, we utilize domain generalization datasets [13]. In particular, this dataset is partitioned into multiple distinct domains, which we use to represent different clients. We assign the retain and forget clients to separate domains to ensure a clear distinction between them. Consequently, when performing client unlearning, we can quantitatively assess the effectiveness of the unlearning process by evaluating model performance on both the retained and forgotten client domains, as well as on the test domain.

Hyperparameters & Datasets & Model. In our experiments, we evaluate the proposed method on four datasets: PACS [23], VLCS [14], OfficeHome [42], and TerraIncognita [3]. Each dataset contains four distinct domains (i.e.,

Photo, Art, Sketch, and Cartoon for PACS, and Art, Clipart, Product, and Real-World for OfficeHome). We adopt ResNet-18 as the backbone network for PACS, OfficeHome, VLCS, and ResNet-50 for TerraIncognita. All experiments are conducted on a single NVIDIA A100 GPU. To simulate the FL environment, we consider $U = 20$ clients under an IID setting. The clients are divided across the 4 domains, with 5 clients assigned to each domain. For the FUL experiments, we designate clients from one domain as the forget set, while clients from the remaining domains constitute the retain set. The unlearning procedure is then applied to all clients within the forget set.

Implementation Details. For every dataset and model configuration, we initially train a global model using FedAvg until it reaches convergence, after which the proposed unlearning algorithm is applied. In each round, all clients participate according to the designated retain and forget sets. The local dataset of each client is partitioned into training and validation subsets in a 90:10 ratio, while an independent test set is employed to evaluate the model’s performance.

Evaluation Metrics. Following prior works [11, 20], we evaluate the effectiveness and efficiency of FOUL using the following metrics: retain accuracy (RA), forget accuracy (FA), test accuracy (TA), membership inference attack (MIA), communication cost, and computation cost. The retain and forget accuracies measure the model’s performance on the retain and forget dataset $\mathcal{D}_r, \mathcal{D}_f$, respectively. MIA quantifies the extent to which \mathcal{D}_f remain recognizable to the model after unlearning. The retain accuracy reflects how well the model preserves knowledge of \mathcal{D}_r , the forget accuracy evaluates how effectively the model forgets \mathcal{D}_f . Communication and computation costs represent the total amount of data transmitted and the total FLOPs required every communication round during the unlearning process. In addition, we introduce Time-to-Forget (T2F), which measures the average reduction in accuracy on the forget set per round, thereby indicating how quickly the model unlearns the designated clients. To ensure fair evaluation between the retain and forget sets, we assess performance using the global model obtained after each aggregation round and report the average results across all local datasets.

Baselines. We compare the proposed FOUL method with the baselines, including Retraining (in which the model is retrained from scratch using only the retain client set. The resulting aggregated models are then evaluated on both the retain and forget client sets), FATS [41], FedDCP [44], FedRecovery [54], FedOSD [32], FFMU [4], FUSED [56], MoDE [55], and NoT [20].

5. Experimental Evaluation

Main Results. Table 1 presents a comparison of FOUL with other baselines on the PACS and TerraIncognita datasets. The baselines are grouped into two categories: fast

Table 1. Comparison of methods on ResNet-18 with PACS and TerraIncognita datasets. The table reports Forget Accuracy (FA), Remaining Accuracy (RA), Testing Accuracy (TA), and Membership Inference Attack (MIA), with values in parentheses showing the difference from the Retrain baseline. For the FOUL method, (1) corresponds to the L2U phase, and (2) refers to the on-server gradient matching unlearning phase. Note that we **bold** results achieving the closest TA accuracy to Retrain.

Group	Methods	PACS				TerraIncognita			
		FA (↓)	RA (↑)	TA (↑)	MIA (↓)	FA (↓)	RA (↑)	TA (↑)	MIA (↓)
Retrain	Retrain	70.51	82.84	77.45	50.02	30.64	42.41	38.94	50.71
	FATS	74.45 (+3.94)	80.91 (-1.93)	75.98 (-1.47)	55.72 (+5.70)	33.07 (+2.43)	40.96 (-1.45)	37.34 (-1.60)	60.81 (+10.10)
	NoT	73.24 (+2.73)	79.25 (-3.59)	75.28 (-2.17)	59.13 (+9.11)	32.26 (+1.62)	38.32 (-4.09)	36.08 (-2.86)	62.90 (+12.19)
FedCDP	FedCDP	77.37 (+6.86)	78.13 (-4.71)	76.41 (-1.04)	72.26 (+22.24)	34.56 (+3.92)	38.79 (-3.62)	36.75 (-2.19)	81.91 (+31.20)
	FedRecovery	76.48 (+5.97)	76.97 (-5.87)	74.81 (-2.64)	75.24 (+25.22)	32.11 (+1.47)	37.49 (-4.92)	35.59 (-3.35)	84.03 (+33.32)
Approx.	FedOSD	72.89 (+2.38)	80.15 (-2.69)	75.49 (-1.96)	58.84 (+8.82)	32.63 (+1.99)	40.77 (-1.64)	36.76 (-2.18)	60.54 (+9.83)
Unlearn.	FFMU	73.31 (+2.80)	78.27 (-4.57)	74.14 (-3.31)	60.62 (+10.60)	33.76 (+3.12)	39.39 (-3.02)	36.04 (-2.90)	65.85 (+15.14)
	FUSED	75.94 (+5.43)	79.34 (-3.50)	76.86 (-0.59)	58.72 (+8.70)	33.64 (+3.00)	38.73 (-3.68)	36.74 (-2.20)	62.03 (+11.32)
	MoDE	72.53 (+2.02)	79.01 (-3.83)	75.79 (-1.66)	59.79 (+9.77)	32.17 (+1.53)	38.04 (-4.37)	35.74 (-3.20)	63.47 (+12.76)
FOUL	(1)	69.53 (-0.98)	93.11 (+14.55)	77.14 (-0.31)	53.82 (+3.80)	27.97 (-2.67)	43.81 (+1.40)	38.16 (-0.78)	56.40 (+5.69)
	(1) + (2)	70.97 (+0.46)	92.33 (+14.49)	76.43 (-1.02)	51.93 (+1.91)	29.92 (-0.72)	42.13 (-0.28)	39.16 (+0.22)	57.11 (+6.40)

retraining and approximate unlearning. In general, fast retraining methods achieve satisfactory performance in terms of FA and RA. However, they exhibit low T2F, indicating a slower unlearning process. Consequently, these methods suffer from high computational and communication overheads, as well as longer convergence times. Although approximate unlearning methods achieve higher T2F and faster convergence, they generally yield lower FA and RA compared to fast retraining approaches. FOUL consistently outperforms all baselines in client-wise FUL across different architectures and datasets, achieving a smaller average performance gap while maintaining competitive communication and computation costs. The more results on VLCS and OfficeHome datasets are presented in Appendix E.

Time to Forget. Figures 4(a), 5(a), and 6(a) present a comparative analysis of unlearning performance across three approaches: FOUL, retraining with a pre-trained model, and retraining with model reset. The results demonstrate that the two naive retraining methods fail to achieve effective unlearning for the designated forget client set. This limitation arises because both retraining methods employ standard averaging aggregation at the server, which cannot explicitly remove knowledge associated with the forget clients. In contrast, FOUL achieves a substantial reduction in FA, reaching its optimal FA in fewer than 50 rounds, achieving T2F more than 0.32/round (compare to results 75 rounds and T2F of 0.13 of Retraining). Moreover, the RA of FOUL continues to improve during the unlearning phase, indicating that the knowledge of the remaining clients is preserved and not unintentionally unlearned.

Gradient angle and learning properties. Figures 4(b), 5(b), and 6(b) illustrate the average gradient divergence between the retain and forget client sets. This measure is ob-

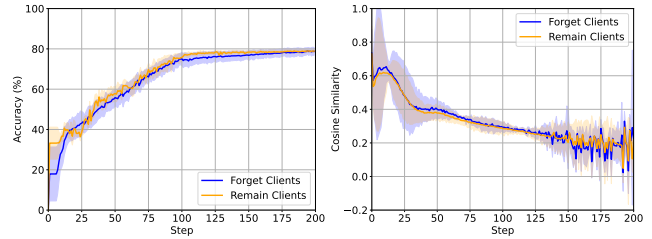


Figure 4. Retaining from scratch with FedAvg without resetting model parameters on PACS dataset.

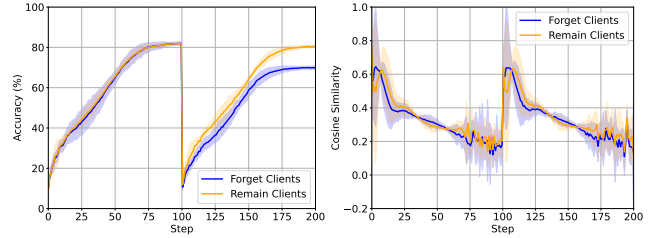


Figure 5. Retaining from scratch with FedAvg with resetting model parameters on PACS dataset.

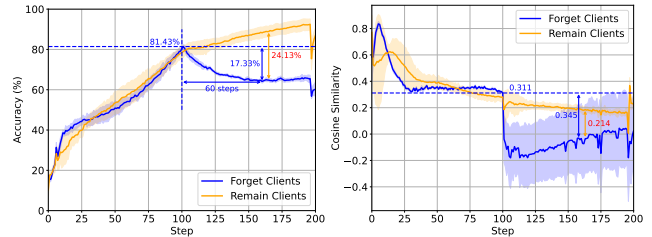


Figure 6. Evaluations of FOUL on PACS dataset.

tained by computing the mean cosine similarity between the global model gradients and those of individual clients in both sets. As shown in Figures 4(b) and 5(b), there is no noticeable difference in gradient divergence between the retain and forget clients, which explains the limited un-

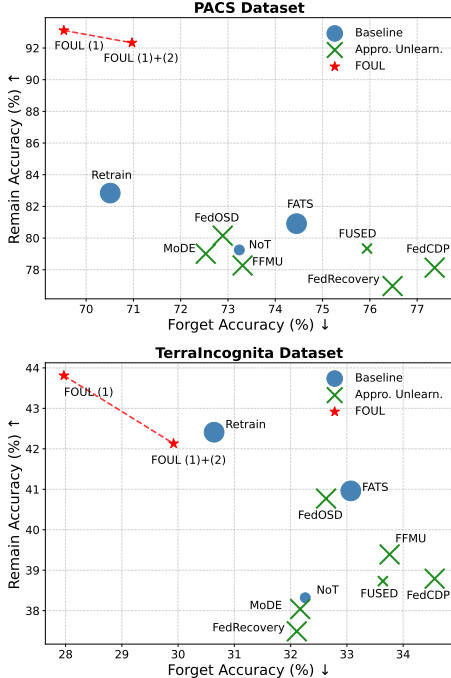


Figure 7. Comparison of communication cost in trade-off with Forget Accuracy (FA) and Remain Accuracy (RA) across different unlearning methods on PACS and TerraIncognita datasets.

learning performance observed in Figures 4(a) and 5(a). In contrast, FOUL exhibits a pronounced reduction in FA that closely corresponds to a decrease in gradient similarity for the forget clients relative to the retain clients. Moreover, the negative cosine similarity values observed for the forget set align with the gradient conflict phenomenon, which has been shown to induce negative transfer effects in multi-task learning [1], domain generalization [33, 36].

Communication & Computation Efficiency. Figure 7 illustrates the communication cost of the FOUL algorithm D compared with other baselines, as well as the trade-off between communication efficiency and RA, FA. As shown in the figure, integrating the L2U stage substantially reduces communication overhead. Moreover, FOUL achieves the highest RA and FA among all compared approaches. As summarized in Table 2, FOUL also demonstrates superior communication and computation efficiency relative to baselines.

6. Ablation Test

Learning to Unlearn Phases To evaluate the impact of the coefficients in the learning-to-unlearn stage of the FOUL algorithm, we conduct a series of experiments, with detailed results and discussions provided in Appendix F. In addition, we assess the domain-invariant capability of

Table 2. Comparison of computational and communication characteristics of each method. Params denotes trainable parameters, Comm. refers to per-round communication overhead, and Comp. indicates local computation complexity.

Method	Params (M)	Comm. (MB)	Comp. (FLOPs)
Retrain	11.3	42.73	$5.81e^{16}$
FATS	11.3	42.73	$5.81e^{16}$
NoT	11.3	34.72	$3.38e^{16}$
FedCDP	11.3	42.73	$5.82e^{16}$
FedRecovery	11.3	42.73	$5.96e^{16}$
FedOSD	11.3	42.73	$5.85e^{16}$
FFMU	11.3	42.73	$5.85e^{16}$
FUSED	11.3	0.98	$2.81e^{16}$
MoDE	11.3	42.73	$3.72e^{16}$
FOUL (1) + (2)	11.3	<u>16.02</u>	$2.35e^{16}$

the proposed model’s disentanglement mechanism, as presented in Appendix G. The results and discussion on the L2U stage with vary causal/non-causal representations dimensionality can be found in Appendix H.

Unlearning Phase To assess the effect of the coefficients used in the unlearning stage of the FOUL algorithm, we perform a series of experiments examining learning rate, sensitivity, and disentanglement efficiency. Results and discussions are provided in Appendix H.

7. Conclusion

This paper addresses the unlearning problem in FL. To overcome key challenges in FUL (including forget-client data inaccessibility, indiscriminate knowledge removal, and high unlearning costs), we propose FOUL, an efficient two-stage framework for learning and unlearning. In the learning stage, the feature extractor is disentangled into two sub-networks: one encoding domain-invariant representations and another capturing domain-variant representations. By restricting the unlearning process to the domain-variant sub-network, FOUL preserves global, task-relevant knowledge across clients while effectively removing features associated with the forget set. In the unlearning stage, on-server gradient matching enables the utilization of both retain and forget client knowledge, significantly improving the time-to-unlearn efficiency. Experimental results demonstrate that FOUL outperforms Retraining in FUL tasks while maintaining communication and computation costs comparable to the standard FedAvg, primarily due to its ability to leverage knowledge from the forget clients.

Acknowledgment

Minh-Duong Nguyen, Le-Tuan Nguyen, Dung D. Le are supported by the Center for AI Research, VinUniversity.

References

- [1] Hao Ban and Kaiyi Ji. Fair resource allocation in multi-task learning. In *International Conference on Machine Learning*, pages 2715–2731. PMLR, 2024. 8
- [2] Adrien Bardes, Jean Ponce, and Yann LeCun. VI-CReg: Variance-invariance-covariance regularization for self-supervised learning. In *ICLR*, 2022. 4
- [3] Sara Beery, Grant Van Horn, and Pietro Perona. Recognition in terra incognita. In *Proceedings of the European conference on computer vision (ECCV)*, pages 456–473, 2018. 6
- [4] Tianshi Che, Yang Zhou, Zijie Zhang, Lingjuan Lyu, Ji Liu, Da Yan, Dejing Dou, and Jun Huan. Fast federated machine unlearning with nonlinear functional theory. In *Proceedings of the 40th International Conference on Machine Learning*, pages 4241–4268. PMLR, 2023. 1, 6
- [5] Gong Cheng, Chunbo Lang, and Junwei Han. Holistic prototype activation for few-shot segmentation. *IEEE Transactions on Pattern Analysis and Machine Intelligence*, 45(4): 4650–4666, 2022. 2
- [6] Vikram S Chundawat, Pushkar Niroula, Prasanna Dhungana, Stefan Schoepf, Murari Mandal, and Alexandra Brintrup. Conda: Fast federated unlearning with contribution dampening. *arXiv*, 2024. 1
- [7] Ningning Ding, Ermin Wei, and Randall Berry. Strategic data revocation in federated unlearning. In *IEEE INFOCOM*, 2024. 1
- [8] Yunfeng Fan, Wenchao Xu, Haozhao Wang, Junxiao Wang, and Song Guo. Pmr: Prototypical modal rebalance for multimodal learning. In *Proceedings of the IEEE/CVF Conference on Computer Vision and Pattern Recognition*, pages 20029–20038, 2023. 2
- [9] Joshua Feinglass, Jayaraman J Thiagarajan, Rushil Anirudh, TS Jayram, and Yezhou Yang. Eyes of a hawk and ears of a fox’: Part prototype network for generalized zero-shot learning. In *Proceedings of the IEEE/CVF conference on computer vision and pattern recognition*, pages 7791–7798, 2024. 2
- [10] Chelsea Finn, Pieter Abbeel, and Sergey Levine. Model-Agnostic Meta-Learning for Fast Adaptation of Deep Networks. In *Asian Conf. Mach. Learn.*, 2017. 2
- [11] Hanlin Gu, WinKent Ong, Chee Seng Chan, and Lixin Fan. Ferrari: federated feature unlearning via optimizing feature sensitivity. *Advances in Neural Information Processing Systems*, 37:24150–24180, 2024. 1, 3, 6
- [12] Hanlin Gu, Hong Xi Tae, Chee Seng Chan, and Lixin Fan. A few-shot label unlearning in vertical federated learning. *arXiv*, 2024. 1
- [13] Ishaan Gulrajani and David Lopez-Paz. In search of lost domain generalization. In *International Conference on Learning Representations*. 6
- [14] Ishaan Gulrajani and David Lopez-Paz. In Search of Lost Domain Generalization. In *ICLR*, 2021. 6, 8
- [15] Weizhao He, Yang Zhang, Wei Zhuo, Linlin Shen, Jiaqi Yang, Songhe Deng, and Liang Sun. Apség: Auto-prompt network for cross-domain few-shot semantic segmentation. In *Proceedings of the IEEE/CVF Conference on Computer Vision and Pattern Recognition*, pages 23762–23772, 2024. 2
- [16] Wenjin Hou, Shiming Chen, Shuhuang Chen, Ziming Hong, Yan Wang, Xuetao Feng, Salman Khan, Fahad Shahbaz Khan, and Xinge You. Visual-augmented dynamic semantic prototype for generative zero-shot learning. In *Proceedings of the IEEE/CVF conference on computer vision and pattern recognition*, pages 23627–23637, 2024. 2
- [17] Wenke Huang, Mang Ye, Zekun Shi, He Li, and Bo Du. Rethinking federated learning with domain shift: A prototype view. In *2023 IEEE/CVF Conference on Computer Vision and Pattern Recognition (CVPR)*, pages 16312–16322. IEEE, 2023. 2
- [18] Zenan Huang, Haobo Wang, Junbo Zhao, and Nenggan Zheng. idag: Invariant dag searching for domain generalization. In *Proceedings of the IEEE/CVF International Conference on Computer Vision*, pages 19169–19179, 2023. 2
- [19] Peiyuan Jia, DeLong Zhang, Lei Zhang, Daojun Han, Juntao Zhang, and Yulong Sang. Prototedla: Prototype guided personalized federated learning based on localized aggregation across heterogeneous clients. In *2024 IEEE International Symposium on Parallel and Distributed Processing with Applications (ISPA)*, pages 196–203. IEEE, 2024. 2
- [20] Yasser H Khalil, Leo Brunswic, Soufiane Lamghari, Xu Li, Mahdi Beitollahi, and Xi Chen. Not: Federated unlearning via weight negation. In *Proceedings of the Computer Vision and Pattern Recognition Conference*, pages 25759–25769, 2025. 1, 3, 6
- [21] Do Khoi, Nguyen Minh-Duong, Le Nam-Khanh, Quoc-Viet Pham, Hua Binh-Son, and Hwang Won-Joo. Domain generalization via pareto optimal gradient matching. In *ECAI*, 2025. 5
- [22] Diederik P Kingma and Max Welling. Auto-Encoding Variational Bayes. *arXiv preprint arXiv:1312.6114*, 2013. 5
- [23] Da Li, Yongxin Yang, Yi-Zhe Song, and Timothy M Hospedales. Deeper, broader and artier domain generalization. In *Proceedings of the IEEE international conference on computer vision*, pages 5542–5550, 2017. 6
- [24] Ya Li, Xinmei Tian, Mingming Gong, Yajing Liu, Tongliang Liu, Kun Zhang, and Dacheng Tao. Deep Domain Generalization via Conditional Invariant Adversarial Networks. In *ECCV*, 2018. 2
- [25] Gaoyang Liu, Xiaoqiang Ma, Yang Yang, Chen Wang, and Jiangchuan Liu. Federaser: Enabling efficient client-level data removal from federated learning models. In *2021 IEEE/ACM 29th International Symposium on Quality of Service (IWQoS)*, 2021. 1
- [26] Jie Liu, Yanqi Bao, Guo-Sen Xie, Huan Xiong, Jan-Jakob Sonke, and Efstratios Gavves. Dynamic prototype convolution network for few-shot semantic segmentation. In *Proceedings of the IEEE/CVF conference on computer vision and pattern recognition*, pages 11553–11562, 2022. 2
- [27] Yi Liu, Lei Xu, Xingliang Yuan, Cong Wang, and Bo Li. The right to be forgotten in federated learning: An efficient realization with rapid retraining. In *IEEE INFOCOM*, 2022. 1
- [28] Chaochao Lu, Yuhuai Wu, José Miguel Hernández-Lobato, and Bernhard Schölkopf. Invariant causal representation

- learning for out-of-distribution generalization. In *International Conference on Learning Representations*, 2021. 2
- [29] Fangrui Lv, Jian Liang, Shuang Li, Bin Zang, Chi Harold Liu, Ziteng Wang, and Di Liu. Causality inspired representation learning for domain generalization. In *CVPR*, 2022. 3, 2
- [30] Trong Binh Nguyen, Duong Minh Nguyen, Jinsun Park, Viet Quoc Pham, and Won-Joo Hwang. Federated domain generalization with data-free on-server gradient matching. In *The Thirteenth International Conference on Learning Representations*, 2025. 5
- [31] Alex Nichol, Joshua Achiam, and John Schulman. On First-Order Meta-Learning Algorithms. *arXiv preprint arXiv:1803.02999*, 2018. 2
- [32] Zibin Pan, Zhichao Wang, Chi Li, Kaiyan Zheng, Boqi Wang, Xiaoying Tang, and Junhua Zhao. Federated unlearning with gradient descent and conflict mitigation. In *Proceedings of the AAAI Conference on Artificial Intelligence*, pages 19804–19812, 2025. 6, 1
- [33] Alexandre Rame, Corentin Dancette, and Matthieu Cord. Fishr: Invariant gradient variances for out-of-distribution generalization. In *Asian Conf. Mach. Learn.*, pages 18347–18377, 2022. 8
- [34] Protection Regulation. General data protection regulation. *Intouch*, 25:1–5, 2018. 1
- [35] Mohammad Saeed Ebrahimi Saadabadi, Ali Dabouei, Sahar Rahimi Malakshan, and Nasser M Nasrabadi. Hyperspherical classification with dynamic label-to-prototype assignment. In *Proceedings of the IEEE/CVF Conference on Computer Vision and Pattern Recognition*, pages 17333–17342, 2024. 2
- [36] Yuge Shi, Jeffrey Seely, Philip Torr, Siddharth N, Awani Hannun, Nicolas Usunier, and Gabriel Synnaeve. Gradient matching for domain generalization. In *ICLR*, 2022. 5, 8
- [37] Jake Snell, Kevin Swersky, and Richard Zemel. Prototypical networks for few-shot learning. In *NeurIPS*, 2017. 4, 1
- [38] Ningxin Su and Baochun Li. Asynchronous federated unlearning. In *IEEE INFOCOM*, 2023. 1
- [39] Yue Tan, Guodong Long, Jie Ma, Lu Liu, Tianyi Zhou, and Jing Jiang. Federated learning from pre-trained models: A contrastive learning approach. *Advances in neural information processing systems*, 35:19332–19344, 2022. 2
- [40] Feilong Tang, Zhongxing Xu, Zhaojun Qu, Wei Feng, Xingjian Jiang, and Zongyuan Ge. Hunting attributes: Context prototype-aware learning for weakly supervised semantic segmentation. In *Proceedings of the IEEE/CVF Conference on Computer Vision and Pattern Recognition*, pages 3324–3334, 2024. 2
- [41] Youming Tao, Cheng-Long Wang, Miao Pan, Dongxiao Yu, Xiuzhen Cheng, and Di Wang. Communication efficient and provable federated unlearning. *Proc. VLDB Endow.*, 2024. 6, 1
- [42] Hemanth Venkateswara, Jose Eusebio, Shayok Chakraborty, and Sethuraman Panchanathan. Deep hashing network for unsupervised domain adaptation. In *Proceedings of the IEEE conference on computer vision and pattern recognition*, pages 5018–5027, 2017. 6
- [43] Junxiao Wang, Song Guo, Xin Xie, and Heng Qi. Federated unlearning via class-discriminative pruning. In *Proc. ACM Web Conf.*, 2022. 1
- [44] Junxiao Wang, Song Guo, Xin Xie, and Heng Qi. Federated unlearning via class-discriminative pruning. In *Proceedings of the ACM web conference 2022*, pages 622–632, 2022. 6
- [45] Lei Wang, Jieming Bian, Letian Zhang, Chen Chen, and Jie Xu. Taming cross-domain representation variance in federated prototype learning with heterogeneous data domains. *Advances in Neural Information Processing Systems*, 37: 88348–88372, 2024. 2
- [46] Pengfei Wang, Zongzheng Wei, Heng Qi, Shaohua Wan, Yunming Xiao, Geng Sun, and Qiang Zhang. Mitigating poor data quality impact with federated unlearning for human-centric metaverse. *IEEE Journal on Selected Areas in Communications*, 2024. 1
- [47] Zichen Wang, Xiangshan Gao, Cong Wang, Peng Cheng, and Jiming Chen. Efficient vertical federated unlearning via fast retraining. *ACM Trans. Internet Technol.*, 2024. 1
- [48] Hui Xia, Shuo Xu, Jiaming Pei, Rui Zhang, Zhi Yu, Weitao Zou, Lukun Wang, and Chao Liu. Fedme2: Memory evaluation & erase promoting federated unlearning in dtmn. *IEEE Jour. of Sel. Areas in Comm.*, 2023. 1
- [49] Heng Xu, Tianqing Zhu, Lefeng Zhang, Wanlei Zhou, and Philip S. Yu. Update selective parameters: Federated machine unlearning based on model explanation. *IEEE Trans. on Big Data*, 2024. 2, 1
- [50] Yanli Yuan, Bingbing Wang, Chuan Zhang, Zehui Xiong, Chunhai Li, and Liehuang Zhu. Toward efficient and robust federated unlearning in iot networks. *IEEE Internet of Things Journal*, 2024. 1
- [51] Hui Zhang, Zuxuan Wu, Zheng Wang, Zhineng Chen, and Yu-Gang Jiang. Prototypical residual networks for anomaly detection and localization. In *Proceedings of the IEEE/CVF Conference on Computer Vision and Pattern Recognition*, pages 16281–16291, 2023. 2
- [52] Jianqing Zhang, Yang Hua, Hao Wang, Tao Song, Zhengui Xue, Ruhui Ma, Jian Cao, and Haibing Guan. Gpfl: Simultaneously learning global and personalized feature information for personalized federated learning. In *Proceedings of the IEEE/CVF international conference on computer vision*, pages 5041–5051, 2023. 2
- [53] Jianqiao Zhang, Caifeng Shan, and Jungong Han. Fedgmkd: An efficient prototype federated learning framework through knowledge distillation and discrepancy-aware aggregation. *Advances in Neural Information Processing Systems*, 37: 118326–118356, 2024. 2
- [54] Lefeng Zhang, Tianqing Zhu, Haibin Zhang, Ping Xiong, and Wanlei Zhou. Fedrecovery: Differentially private machine unlearning for federated learning frameworks. *IEEE Transactions on Information Forensics and Security*, 18: 4732–4746, 2023. 6
- [55] Yian Zhao, Pengfei Wang, Heng Qi, Jianguo Huang, Zongzheng Wei, and Qiang Zhang. Federated unlearning with momentum degradation. *IEEE Internet of Things Journal*, 2024. 6, 1

- [56] Zhengyi Zhong, Weidong Bao, Ji Wang, Shuai Zhang, Jingxuan Zhou, Lingjuan Lyu, and Wei Yang Bryan Lim. Unlearning through knowledge overwriting: Reversible federated unlearning via selective sparse adapter. In *Proceedings of the Computer Vision and Pattern Recognition Conference*, pages 30661–30670, 2025. [3](#), [6](#), [1](#)
- [57] Fei Zhou, Peng Wang, Lei Zhang, Wei Wei, and Yanning Zhang. Revisiting prototypical network for cross domain few-shot learning. In *Proceedings of the IEEE/CVF conference on computer vision and pattern recognition*, pages 20061–20070, 2023. [2](#)
- [58] Tianfei Zhou and Wenguan Wang. Prototype-based semantic segmentation. *IEEE Transactions on Pattern Analysis and Machine Intelligence*, 46(10):6858–6872, 2024. [2](#)
- [59] Tianfei Zhou, Wenguan Wang, Ender Konukoglu, and Luc Van Gool. Rethinking semantic segmentation: A prototype view. In *Proceedings of the IEEE/CVF conference on computer vision and pattern recognition*, pages 2582–2593, 2022. [2](#)

Computation and Communication Efficient Federated Unlearning via On-server Gradient Conflict Mitigation and Expression

Supplementary Material

A. Related Works

A.1. Federated Unlearning

Recently, there have been some FUL approaches, including 1) fast retraining, and 2) approximate unlearning.

Fast retraining: To design a fast training protocol for FUL, [7, 47] propose user data revocation strategies to ensure the efficient unlearning process among users in FL system. FedEraser [25] initiates the unlearning algorithm among the clients that request data removal. However, other clients' models still hold the contributions of the data to be removed, which will be later aggregated in a global model. To address this, their proposed solution uses the latest rounds of local model updates to approximate the current unlearned model update. Nonetheless, if the data samples to be removed have been used for training from the beginning, the model updates may still contain traces of these samples. [27] introduces a fast retraining approach by leveraging the diagonals of Fisher Information Matrix (FIM). This approach significantly improves the efficiency of the approximation of inverse Hessian. KNOT [38] proposes a clustered FL concept to improve the efficiency of retraining in FUL. Specifically, due to the clustered aggregation mechanism, the FUL concept using KNOT only has to retrain a partial set of clients, thus improving the retraining efficiency in FUL. NoT [20] introduces a weight negation operator that perturbs the model parameters away from their optimal values, thereby positioning the model more favorably for subsequent re-training.

Approximate Unlearning FATS [41] evaluates the involvement of clients in the previous training of the federated learning (FL) system. Consequently, the contributions of clients are considered accordingly in the unlearning stage. MetaFUL [46] proposes an efficient unlearning algorithm that leverages the impact of user data, which is measured during the learning stage. MoDe [55] applies slow-update techniques in federated unlearning to improve the smoothness of the unlearning process, thereby enhancing overall performance. However, the naive unlearning approach (i.e., excluding clients with revocation requests from the aggregation stage) does not ensure a reduced generalization gap between conventional machine unlearning and FUL. FedRemover [50] introduces a two-step approach for unlearning malicious clients, which includes: 1) attack detection, and 2) gradient direction analysis-based malicious

client identification. This method significantly improves energy and computational efficiency in identifying clients for unlearning. FFMU [4] employs quantization on local models, demonstrating that it can efficiently unlearn knowledge from the set of forget devices. The authors in [43] propose a TF-IDF Guided Pruning approach for efficient FUL. Specifically, the server uses TF-IDF, a statistical measure of channel impact on class discrimination, to determine which network channels should be pruned. However, this pruning-based approach not only removes information about the unlearning classes but also erases information from some remaining data, leading to a degradation in data discrimination.

To address this issue, [49] proposes an on-server unlearning process for FUL. However, this method requires on-server data, which negatively impacts the communication efficiency of the FL system. Conda [6] introduces an on-server unlearning method that identifies global model parameter sets most affected by forget clients. By dampening these parameters, Conda achieves effective unlearning while preserving the rest of the model parameters on the server side. FUSED [56] identifies the critical layers that contribute most to learning and performs updates selectively on these layers through a sparse update strategy. This approach significantly reduces the computational cost required during the unlearning phase.

The authors in [12] propose a mixup-based strategy to enrich the data used in unlearning. Ferrari [11] introduces a new metric for feature-level unlearning called feature sensitivity. FedME2 [48] presents an FUL architecture with two key components: 1) memory evaluation (MEval), and 2) erasure (MErase). MEval follows the rationale that the informational bottleneck significantly reduces redundant information from the data. By evaluating the final layers, it determines whether data is efficiently remembered within the model architecture. The authors design an evaluation loss function for the federated unlearning problem, thereby efficiently improving the performance of federated unlearning. FedOSD [32] enables client-side unlearning by incorporating an unlearning cross-entropy loss to remove undesired knowledge locally, and adopts gradient surgery to ensure gradient alignment among heterogeneous clients.

A.2. Prototype Learning

Prototype learning [37] has emerged as a powerful paradigm for classification tasks, where models learn representative embeddings, or prototypes, for each class. A

prototype typically refers to the mean feature vector of instances belonging to the same class [24]. Beyond serving as a classification tool, prototype learning can also be viewed as an implicit form of causal factor discovery, as each prototype may correspond to a distinct causal factor in the underlying CSM [18, 29].

In supervised classification, a query sample is classified by measuring its distance to the prototypes of each class, which has been shown to yield more robust and stable performance [35, 51], particularly in few-shot [5, 15, 26, 57] and zero-shot learning [9, 16] settings. Moreover, prototype-based approaches have gained increasing attention in semantic segmentation [58, 59], multimodal learning [8] and unsupervised representation learning [40].

In the context of FL, prototypes can serve as a compact and privacy-preserving form of abstract knowledge that enables efficient information sharing among clients. Recent studies have integrated prototype learning into FL frameworks to address data heterogeneity across clients [39, 53], mitigate domain shift [17, 45], and enhance personalization in local models [19, 39, 52].

B. Two-stage Optimization for learning stage of FOUL

The joint loss function is complex which makes the optimization problem NP-hard. Acknowledging this shortcoming, we decompose the FOUL training process into two steps, denoted as the *L2U Generator* and the *Meaningful Invariant Discriminator* (MID). The *L2U Generator* is responsible for training the featurizer to achieve good data reconstruction while maintaining the invariant and variant characteristics of z_K and z_V , respectively. The *MID* focuses on distilling essential knowledge into the invariant representation z_K . By splitting the complicated tasks into two simpler tasks with fewer loss components, the individual tasks become significantly more straightforward, thereby enhancing the overall training process. To train these two disentangled tasks jointly and efficiently, we use a cost-effective meta-learning technique called Reptile [31]. Reptile is proven to be computationally efficient while maintaining performance comparable to conventional meta-learning approaches [10]. In our Reptile-based L2U, the *L2U Generator* and *MID* are trained alternately in a continuous manner. At the start of each training round r , we begin with the *L2U Generator* to prioritize the training of meaningful representations that can be faithfully reconstructed. Specifically, the

Algorithm 1: Pseudo algorithm for L2U stage of FOUL.

```

1 Input: Initial model parameter  $\theta_0$ , learning
   coefficients  $\alpha_{\text{rec}}, \alpha_v, \alpha_{\text{iv}}, \alpha_{\text{gtc}}, \alpha_{\text{adv}} \in [0, 1]$  and
   learning rate  $\eta_{\text{L2U}}, \eta_{\text{MID}}, \eta_{\text{adv}} \in \mathbb{R}^+$ . Local
   iterations  $E = I_{\text{L2U}} + I_{\text{MID}}$ 
2 for training round  $r = 0, 1, \dots, I$  do
3   /* Local Training */
4   for client  $u \in \mathcal{U}$  do
5     /* L2U Generator */
6     for iteration  $i = 0, 1, \dots, I_{\text{L2U}} - 1$  do
7       Compute loss for the representation
         disentanglement:
           
$$\mathcal{L}_{\text{L2U}} = \alpha_{\text{rec}}\mathcal{L}_{\text{rec}} + \alpha_{\text{iv}}\mathcal{L}_{\text{iv}} + \alpha_v\mathcal{L}_v.$$

8       Apply gradient descent according
         to Eq. (11).
9     end for
10    /* Meaningful Invariant Discriminator */
11    for iteration  $i = I_{\text{L2U}}, \dots, I_{\text{L2U}} + I_{\text{MID}}$  do
12      Compute loss for meaningful invariant
        representation:
          
$$\mathcal{L}_{\text{MID}} = \alpha_{\text{iv}}\mathcal{L}_{\text{iv}} + \alpha_{\text{gtc}}\mathcal{L}_{\text{gtc}}.$$

13      Apply gradient descent according
        to Eq. (12).
14    end for
15    Upload local model  $\theta_u^{(r,E)}$  to the server.
16  end for
17  /* Global Aggregation */
18  Compute global model  $\theta_g^{(r)} = \sum_{u \in \mathcal{U}} \theta_u^{(r,E)}$ .
19 end for

```

L2U model is updated within the *L2U Generator* as follows:

$$\begin{aligned}
\theta_E^{r,i+1} &= \theta_E^{r,i} - \eta_{\text{L2U}} \nabla_{\theta_E^{r,i}} \mathcal{L}_{\text{L2U}}, \\
\theta_V^{r,i+1} &= \theta_V^{r,i} - \eta_{\text{L2U}} \nabla_{\theta_V^{r,i}} \mathcal{L}_{\text{L2U}}, \\
\theta_K^{r,i+1} &= \theta_K^{r,i} - \eta_{\text{L2U}} \nabla_{\theta_K^{r,i}} \mathcal{L}_{\text{L2U}}, \\
\theta_2^{r,i+1} &= \theta_2^{r,i} - \eta_{\text{L2U}} \nabla_{\theta_2^{r,i}} \mathcal{L}_{\text{L2U}}.
\end{aligned} \tag{11}$$

In the subsequent *MID*, we focus on the training of featurizers θ_E, θ_K and finetune the label classifier θ_{gtc} as follows:

$$\begin{aligned}
\theta_E^{r,i+1} &= \theta_E^{r,i} - \eta_{\text{MID}} \nabla_{\theta_E^{r,i}} \mathcal{L}_{\text{MID}}^{r,i}, \\
\xi^{r,i+1} &= \xi^{r,i} - \eta_{\text{MID}} \nabla_{\theta_{\text{gtc}}^{r,i}} \mathcal{L}_{\text{MID}}^{r,i}.
\end{aligned} \tag{12}$$

The details of the training process are shown in Algorithm 1.

C. Client-level Federated Unlearning Derivation

Theorem 1 (FOUL solution) Given $\Gamma = \{\gamma_u^{(r)} | u \in \mathcal{U}, \sum_{u \in \mathcal{U}} \gamma_u^{(r)} = 1\}$ is the set of learnable coefficients at each round r . Invariant gradient direction $g_{\text{UL}}^{(r)}$ is characterized as follows:

$$g_{\text{UL}}^{(r)} = g_{\text{FL}}^{(r)} + \frac{\kappa \|g_{\text{FL}}^{(r)}\|}{\|g_{\Gamma_{\mathcal{R}}}^{(r)} - g_{\Gamma_{\mathcal{F}}}^{(r)}\|} (g_{\Gamma_{\mathcal{R}}}^{(r)} - g_{\Gamma_{\mathcal{F}}}^{(r)}), \quad (13)$$

s.t. $\Gamma_{\mathcal{R}}^*, \Gamma_{\mathcal{F}}^* = \arg \min_{\Gamma_{\mathcal{R}}, \Gamma_{\mathcal{F}}} (g_{\Gamma_{\mathcal{R}}}^{(r)} - g_{\Gamma_{\mathcal{F}}}^{(r)}) \cdot g_{\text{FL}}^{(r)} + \sqrt{\kappa} \|g_{\text{FL}}^{(r)}\| \|g_{\Gamma_{\mathcal{R}}}^{(r)} - g_{\Gamma_{\mathcal{F}}}^{(r)}\|.$

Proof. We consider $x = g_{\text{UL}}^{(r)}$ and consider the maximization problem with x as optimization variable. Denote $\phi = \kappa^2 \|g_{\text{FL}}^{(r)}\|^2$. Note that $\min_u \langle g_u^{(r)}, g_{\text{FL}}^{(r)} \rangle = \min_{\gamma} \langle \sum_u \gamma_u h_u^{(r)}, h_g^{(r)} \rangle$. The Lagrangian of the objective is

$$\max_x \min_{\lambda, \gamma} \left(\sum_{u \in \mathcal{U}_{\mathcal{R}}} \gamma_u h_u^{(r)} \right)^\top x - \beta \left(\sum_{v \in \mathcal{U}_{\mathcal{F}}} \gamma_v h_v^{(r)} \right)^\top x - \frac{\lambda}{2} \|g_{\text{FL}}^{(r)} - x\|^2 + \frac{\lambda}{2} \phi, \quad \text{s.t. } \lambda \geq 0. \quad (14)$$

Since the problem is a convex programming and Slater's condition is satisfied for $\kappa > 0$ (meanwhile, if $\kappa = 0$, it can be easily verified that all results hold trivially), the strong duality holds. Consequently, the order of the min and max operations can be interchanged. For instance,

$$\min_{\lambda, \gamma} \max_x \underbrace{\left(\sum_{u \in \mathcal{U}_{\mathcal{R}}} \gamma_u h_u^{(r)} \right)^\top x - \beta \left(\sum_{v \in \mathcal{U}_{\mathcal{F}}} \gamma_v h_v^{(r)} \right)^\top x - \frac{\lambda}{2} \|g_{\text{FL}}^{(r)} - x\|^2 + \frac{\lambda}{2} \phi}_{A_1}, \quad \text{s.t. } \lambda \geq 0. \quad (15)$$

Taking A_1 into consideration. If we consider λ, γ as constant, x is the variable, x achieves the optimal solution when $\partial A_1 / \partial x = 0$. Thus, we have the followings:

$$\frac{\partial A_1}{\partial x} = \sum_{u \in \mathcal{U}_{\mathcal{R}}} \gamma_u h_u^{(r)} - \beta \sum_{v \in \mathcal{U}_{\mathcal{F}}} \gamma_v h_v^{(r)} - \lambda(x - g_{\text{FL}}^{(r)}) = 0. \quad (16)$$

Another speaking, we have

$$x = g_{\text{FL}}^{(r)} + \left(\sum_{u \in \mathcal{U}_{\mathcal{R}}} \gamma_u h_u^{(r)} - \beta \sum_{v \in \mathcal{U}_{\mathcal{F}}} \gamma_v h_v^{(r)} \right) / \lambda. \quad (17)$$

Therefore, we have the followings:

$$A_1 = \left(\sum_{u \in \mathcal{U}_{\mathcal{R}}} \gamma_u h_u^{(r)} \right)^\top \left(g_{\text{FL}}^{(r)} + \left(\sum_{u \in \mathcal{U}_{\mathcal{R}}} \gamma_u h_u^{(r)} - \beta \sum_{v \in \mathcal{U}_{\mathcal{F}}} \gamma_v h_v^{(r)} \right) / \lambda \right) - \beta \left(\sum_{v \in \mathcal{U}_{\mathcal{F}}} \gamma_v h_v^{(r)} \right)^\top \left(g_{\text{FL}}^{(r)} + \left(\sum_{u \in \mathcal{U}_{\mathcal{R}}} \gamma_u h_u^{(r)} - \beta \sum_{v \in \mathcal{U}_{\mathcal{F}}} \gamma_v h_v^{(r)} \right) / \lambda \right) - \frac{1}{2\lambda} \left\| \sum_{u \in \mathcal{U}_{\mathcal{R}}} \gamma_u h_u^{(r)} - \beta \sum_{v \in \mathcal{U}_{\mathcal{F}}} \gamma_v h_v^{(r)} \right\|^2 + \frac{\lambda}{2} \phi. \quad (18)$$

Substituting $g_{\Gamma_{\mathcal{R}}}^{(r)} = \sum_{u \in \mathcal{U}_{\mathcal{R}}} \gamma_u h_u^{(r)}$ and $g_{\Gamma_{\mathcal{F}}}^{(r)} = \sum_{v \in \mathcal{U}_{\mathcal{F}}} \gamma_v h_v^{(r)}$. Consider the optimization problem of Eq. (18), we have:

$$\begin{aligned} A_1 &= g_{\Gamma_{\mathcal{R}}}^{(r)\top} \left(g_{\text{FL}}^{(r)} + (g_{\Gamma_{\mathcal{R}}}^{(r)} - \beta g_{\Gamma_{\mathcal{F}}}^{(r)}) / \lambda \right) - \beta g_{\Gamma_{\mathcal{F}}}^{(r)\top} \left(g_{\text{FL}}^{(r)} + (g_{\Gamma_{\mathcal{R}}}^{(r)} - \beta g_{\Gamma_{\mathcal{F}}}^{(r)}) / \lambda \right) - \frac{1}{2\lambda} \|g_{\Gamma_{\mathcal{R}}}^{(r)} - \beta g_{\Gamma_{\mathcal{F}}}^{(r)}\|^2 + \frac{\lambda}{2} \phi \\ &= (g_{\Gamma_{\mathcal{R}}}^{(r)} - \beta g_{\Gamma_{\mathcal{F}}}^{(r)})^\top g_{\text{FL}}^{(r)} + \frac{1}{\lambda} (g_{\Gamma_{\mathcal{R}}}^{(r)} - \beta g_{\Gamma_{\mathcal{F}}}^{(r)})^\top (g_{\Gamma_{\mathcal{R}}}^{(r)} - \beta g_{\Gamma_{\mathcal{F}}}^{(r)}) - \frac{1}{2\lambda} \|g_{\Gamma_{\mathcal{R}}}^{(r)} - \beta g_{\Gamma_{\mathcal{F}}}^{(r)}\|^2 + \frac{\lambda}{2} \phi \\ &= (g_{\Gamma_{\mathcal{R}}}^{(r)} - \beta g_{\Gamma_{\mathcal{F}}}^{(r)})^\top g_{\text{FL}}^{(r)} + \frac{1}{2\lambda} \|g_{\Gamma_{\mathcal{R}}}^{(r)} - \beta g_{\Gamma_{\mathcal{F}}}^{(r)}\|^2 + \frac{\lambda}{2} \phi. \end{aligned} \quad (19)$$

Therefore, we have Eq. 15 is equivalent to

$$\min_{\lambda, \gamma} \underbrace{(g_{\Gamma_{\mathcal{R}}}^{(r)} - \beta g_{\Gamma_{\mathcal{F}}}^{(r)})^\top g_{\text{FL}}^{(r)} + \frac{1}{2\lambda} \|g_{\Gamma_{\mathcal{R}}}^{(r)} - \beta g_{\Gamma_{\mathcal{F}}}^{(r)}\|^2 + \frac{\lambda}{2} \phi}_{A_2}. \quad (20)$$

Next, we consider λ as variable to find the optimal value. Subsequently, optimization problem Eq. (20) is equivalent to the following relationship:

$$\frac{\partial}{\partial \lambda} A_2 = -\frac{1}{2\lambda^2} \|g_{\Gamma_{\mathcal{R}}}^{(r)} - \beta g_{\Gamma_{\mathcal{F}}}^{(r)}\|^2 + \frac{1}{2}\phi = 0. \quad (21)$$

Therefore, the equation achieves the optimality as $\lambda = \|g_{\Gamma_{\mathcal{R}}}^{(r)} - g_{\Gamma_{\mathcal{F}}}^{(r)}\|/\phi^{1/2}$. Combining with Eq. (20) and Eq. (17), we have the followings:

$$g_{\text{UL}}^{(r)} = g_{\text{FL}}^{(r)} + \frac{\kappa \|g_{\text{FL}}^{(r)}\|}{\|g_{\Gamma_{\mathcal{R}}}^{(r)} - \beta g_{\Gamma_{\mathcal{F}}}^{(r)}\|} (g_{\Gamma_{\mathcal{R}}}^{(r)} - \beta g_{\Gamma_{\mathcal{F}}}^{(r)}), \quad (22)$$

s.t. $\Gamma_{\mathcal{R}}^*, \Gamma_{\mathcal{F}}^* = \arg \min_{\Gamma_{\mathcal{R}}, \Gamma_{\mathcal{F}}} (g_{\Gamma_{\mathcal{R}}}^{(r)} - \beta g_{\Gamma_{\mathcal{F}}}^{(r)}) \cdot g_{\text{FL}}^{(r)} + \sqrt{\kappa} \|g_{\text{FL}}^{(r)}\| \|g_{\Gamma_{\mathcal{R}}}^{(r)} - \beta g_{\Gamma_{\mathcal{F}}}^{(r)}\|.$

This solves the problem.

D. Pseudo Algorithm for unlearning stage of FOUL

Algorithm 2: Unlearning Stage via On-server Matching Gradient

Input: set of retain users $\mathcal{U}_{\mathcal{R}}$, forget users $\mathcal{U}_{\mathcal{F}}$, $\mathcal{U} = \{\mathcal{U}_{\mathcal{R}}, \mathcal{U}_{\mathcal{F}}\}$, number of communication rounds R , local learning rate η , global learning rate η_g , searching space hyper-parameter κ .

Output: $\theta_{V,g}^{(R)}$

1 **Clients Update:**

2 **for** client $u \in \mathcal{U}$ **do**

3 **Receive** global non-causal encoder $\theta_{V,u}^{(r)} = \theta_{V,g}^{(r)}$;

4 Merge global non-causal encoder $\theta_{V,u}^{(r)}$ into local model $\theta_u^{(r)}$;

5 **for** local epoch $e \in E$ **do**

6 Sample mini-batch ζ from local data \mathcal{D}_u ;

7 Calculate gradient $\nabla_{\theta_{V,u}^{(r,e)}} \mathcal{E}(\theta_u^{(r,e)}, \zeta)$;

8 Update client's non-causal encoder: $\theta_{V,u}^{(r,e+1)} = \theta_{V,u}^{(r,e)} - \eta \nabla_{\theta_{V,u}^{(r,e)}} \mathcal{E}(\theta_u^{(r,e)}, \zeta)$;

9 **end for**

10 Upload client's non-causal encoder $\theta_{V,u}^{(r,E)}$ to server.

11 **end for**

12 **Server Optimization:**

13 **for** round $r = 0, \dots, R$ **do**

14 **Clients Updates;**

15 Calculate $g_u^{(r)} = \theta_{V,u}^{(r,E)} - \theta_{V,u}^{(r)}$, $\mathbf{g}^{(r)} = \{g_u^{(r)} | u \in \mathcal{U}\}$;

16 Calculate $g_{FL}^{(r)}$ (e.g., $g_{FL}^{(r)} = \frac{1}{U} \sum_{u=1}^U g_u^{(r)}$ as the FedAvg update);

17 Calculate $g_{\Gamma_{\mathcal{R}}}^{(r)} = \sum_{u \in \mathcal{U}_{\mathcal{R}}} \gamma_u g_u^{(r)}$ as the retain user set update);

18 Calculate $g_{\Gamma_{\mathcal{F}}}^{(r)} = \sum_{v \in \mathcal{U}_{\mathcal{F}}} \gamma_v g_v^{(r)}$ as the forget user set update);

19 Solve for $\Gamma^* = \{\Gamma_{\mathcal{R}}^*, \Gamma_{\mathcal{F}}^*\}$, where $\Gamma_{\mathcal{R}} = \{\gamma_u | u \in \mathcal{U}_{\mathcal{R}}\}$, $\Gamma_{\mathcal{F}} = \{\gamma_v | v \in \mathcal{U}_{\mathcal{F}}\}$:

$$\Gamma_{\mathcal{R}}^*, \Gamma_{\mathcal{F}}^* = \arg \min_{\Gamma_{\mathcal{R}}, \Gamma_{\mathcal{F}}} (g_{\Gamma_{\mathcal{R}}}^{(r)} - g_{\Gamma_{\mathcal{F}}}^{(r)}) \cdot g_{FL}^{(r)} + \sqrt{\kappa} \|g_{FL}^{(r)}\| \|g_{\Gamma_{\mathcal{R}}}^{(r)} - g_{\Gamma_{\mathcal{F}}}^{(r)}\|.$$

20 Update unlearn gradient: $g_{FOUL}^{(r)} = g_{FL}^{(r)} + \frac{\kappa \|g_{FL}^{(r)}\|}{\|g_{\Gamma_{\mathcal{R}}}^{(r)} - g_{\Gamma_{\mathcal{F}}}^{(r)}\|} (g_{\Gamma_{\mathcal{R}}}^{(r)} - g_{\Gamma_{\mathcal{F}}}^{(r)})$.

21 Update the model: $\theta_{V,g}^{(r)} = \theta_{V,g}^{(r-1)} - \eta_g g_{FOUL}^{(r)}$.

22 **end for**

E. Detailed Results

Table 3. Comparison of methods on ResNet-18 with VLCS and OfficeHome datasets. The table reports Forget Accuracy (FA), Remaining Accuracy (RA), Testing Accuracy (TA), and Membership Inference Attack (MIA), with values in parentheses showing the difference from the Retrain baseline. For the FOUL method, (1) corresponds to the L2U phase, and (2) refers to the on-server gradient matching unlearning phase. Note that we **bold** results achieving the closest TA accuracy to Retrain.

Group	Methods	VLCS				OfficeHome			
		FA (↓)	RA (↑)	TA (↑)	MIA (↓)	FA (↓)	RA (↑)	TA (↑)	MIA (↓)
Retrain	Retrain	63.14	73.88	70.16	52.96	45.90	66.32	59.08	47.64
	FATS	66.51 (+3.37)	72.09 (-1.79)	68.62 (-1.54)	58.68 (+5.72)	48.73 (+2.83)	64.05 (-2.27)	58.13 (-0.95)	57.46 (+9.82)
	NoT	65.52 (+2.38)	71.04 (-2.84)	67.83 (-2.33)	61.93 (+8.97)	47.57 (+1.67)	61.51 (-4.81)	56.15 (-2.93)	59.79 (+12.15)
Unlearn.	FedCDP	69.78 (+6.64)	69.95 (-3.93)	68.63 (-1.53)	74.56 (+21.60)	50.07 (+4.17)	61.83 (-4.49)	57.73 (-1.35)	78.06 (+30.42)
	FedRecovery	69.33 (+6.19)	68.79 (-5.09)	67.61 (-2.55)	77.34 (+24.38)	47.65 (+1.75)	60.81 (-5.51)	56.35 (-2.73)	80.41 (+32.77)
	FedOSD	65.74 (+2.60)	71.85 (-2.03)	67.98 (-2.18)	61.52 (+8.56)	47.81 (+1.91)	64.15 (-2.17)	56.96 (-2.12)	57.21 (+9.57)
	FFMU	66.25 (+3.11)	69.75 (-4.13)	66.55 (-3.61)	63.06 (+10.10)	49.72 (+3.82)	62.66 (-3.66)	56.05 (-3.03)	62.79 (+15.15)
	FUSED	68.08 (+4.94)	70.91 (-2.97)	69.81 (-0.35)	60.84 (+7.88)	49.41 (+3.51)	62.55 (-3.77)	57.55 (-1.53)	58.72 (+11.08)
	MoDE	64.93 (+1.79)	70.72 (-3.16)	68.19 (-1.97)	62.28 (+9.32)	48.10 (+2.20)	61.39 (-4.93)	56.44 (-2.64)	60.15 (+12.51)
FOUL	(1)	61.72 (-1.42)	76.78 (+2.90)	68.97 (-1.19)	56.85 (+3.89)	43.69 (-2.21)	67.03 (+0.71)	61.96 (+2.88)	56.53 (+8.89)
	(1) + (2)	62.91 (-0.23)	77.15 (+3.27)	69.10 (-1.06)	55.83 (+2.87)	44.17 (-1.73)	65.78 (-0.54)	60.77 (+1.69)	57.48 (+9.84)

F. Evaluations on convergence of learning phase

As the joint loss function comprises multiple components, it is theoretically challenging to optimize. Therefore, we conduct ablation experiments on VLCS dataset by varying the coefficients of each component in the joint loss function, as illustrated in Figures 8. In each experiment, we fix all other coefficients to 1 while varying only one coefficient at a time. As shown in the figures, the model converges within fewer than 100 training rounds, which is comparable to the convergence behavior of vanilla FL. Moreover, the low invariant and variance losses indicate that the learned disentangled representations closely align with the theoretical expectations, where the causal and non-causal representations exhibit invariant and variant properties, respectively.

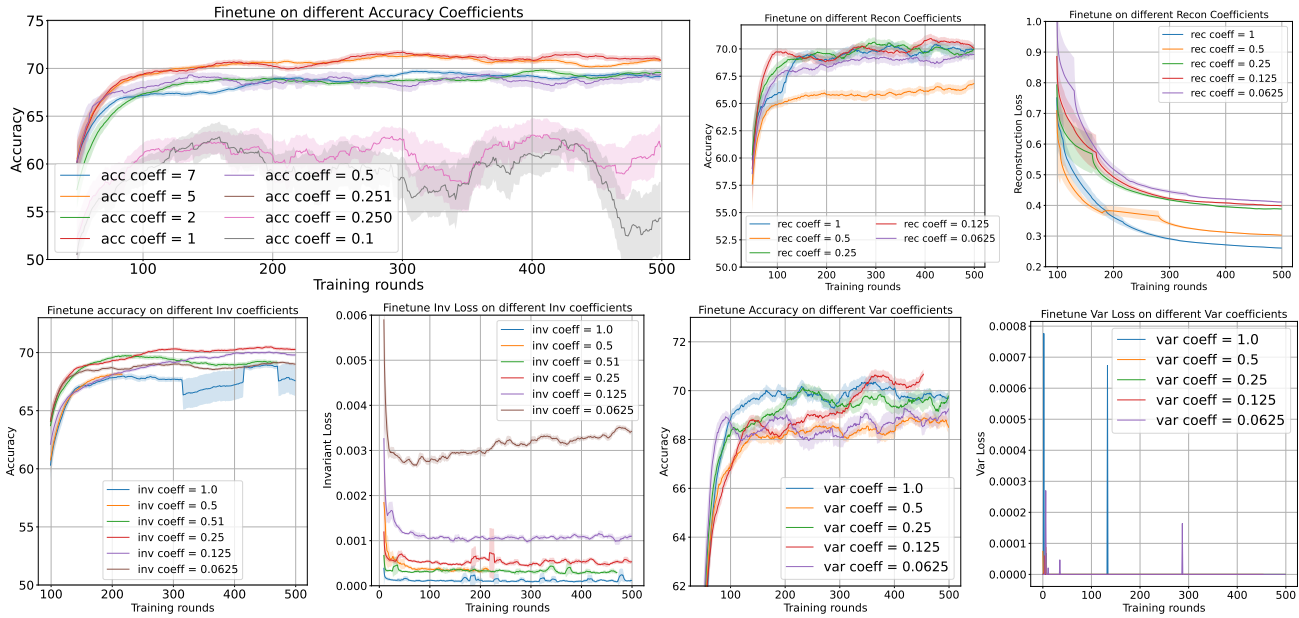


Figure 8. Learning phase of FOUL under different learning coefficient settings.

G. Assessing the domain generalization capabilities of FOUL

We evaluate the performance of FOUL in extracting and predicting invariant representations to verify the robustness of causality-invariant features against domain generalization gaps. To this end, we employ the DomainBed library. Specifically, we train three distinct FOUL models on the Colored-MNIST dataset [14], each using a different domain for training, and subsequently evaluate them on all remaining domains. The results are summarized in Table 4.

Table 4 highlights two key findings. First, the invariant representations z_K capture substantial causal information, enabling accurate prediction of the ground-truth labels in the source domain, which is consistent with the underlying CSM. Second, these invariant representations remain consistent across different data domains. Consequently, by preserving the knowledge of the semantic featurizer during the unlearning phase, FOUL retains the domain-invariant knowledge, ensuring that unlearning on the forget set minimally impacts performance on the retain set.

Table 4. Assessment of FOUL across different domains. The evaluation is conducted on the Colored-MNIST dataset, where each domain corresponds to images with varying degrees of correlation between color and label. Two aspects are assessed: (1) Accuracy: evaluating the model’s ability to predict labels in each domain using only the invariant representations; and (2) Invariance: measuring the disparity between the invariant representations z_K^i generated from a target domain i and those z_K^j obtained from the training domain j , to quantify the consistency of invariant features across domains.

Algorithm	+90%	+80%	-90%
Domain 1 (+90%)			
Accuracy	89.5 ± 0.1	82.3 ± 0.5	73.2 ± 0.3
Invariant	$0.0003 \pm 10e-5$	$0.0002 \pm 10e-5$	$0.0002 \pm 10e-5$
Domain 2 (+80%)			
Accuracy	73.9 ± 0.1	82.3 ± 0.5	73.2 ± 0.3
Invariant	$0.0003 \pm 10e-5$	$0.0002 \pm 10e-5$	$0.0002 \pm 10e-5$
Domain 3 (-90%)			
Accuracy	89.5 ± 0.1	80.7 ± 0.5	73.2 ± 0.3
Invariant	$0.0003 \pm 10e-5$	$0.0002 \pm 10e-5$	$0.0002 \pm 10e-5$

H. Assessment of Knowledge Extraction Capability

To determine the extent of invariant knowledge extraction from the data and the appropriate semantic knowledge size to represent the data from each label, we keep the size of the embedding layer constant (i.e., $C_{IB} = 32$), while simultaneously varying the number of invariant channels and setting the variant channel size to $C_v = C_{IB} - C_{iv}$. This approach is adopted to ensure that the performance of data reconstruction remains unaffected by the informational bottleneck. The results evaluated on VLCS dataset are shown in Fig. 9. As can be seen, the L2U stage performs optimally when the number of invariant knowledge channels are set to $C \geq 16$. Additionally, the data reconstruction remains consistent as the invariant knowledge size is increased. This indicates that higher data reconstruction efficiency can be achieved by using a larger invariant knowledge size (e.g., $C_{iv} \geq 24, C_{Var} \leq 8$). This also implies that a high compression ratio of $(3 \times 32 \times 32) : (8 \times 64) = 6 : 1$ can be attained without quality loss in the variant data, which needs to be transmitted over the physical channel.

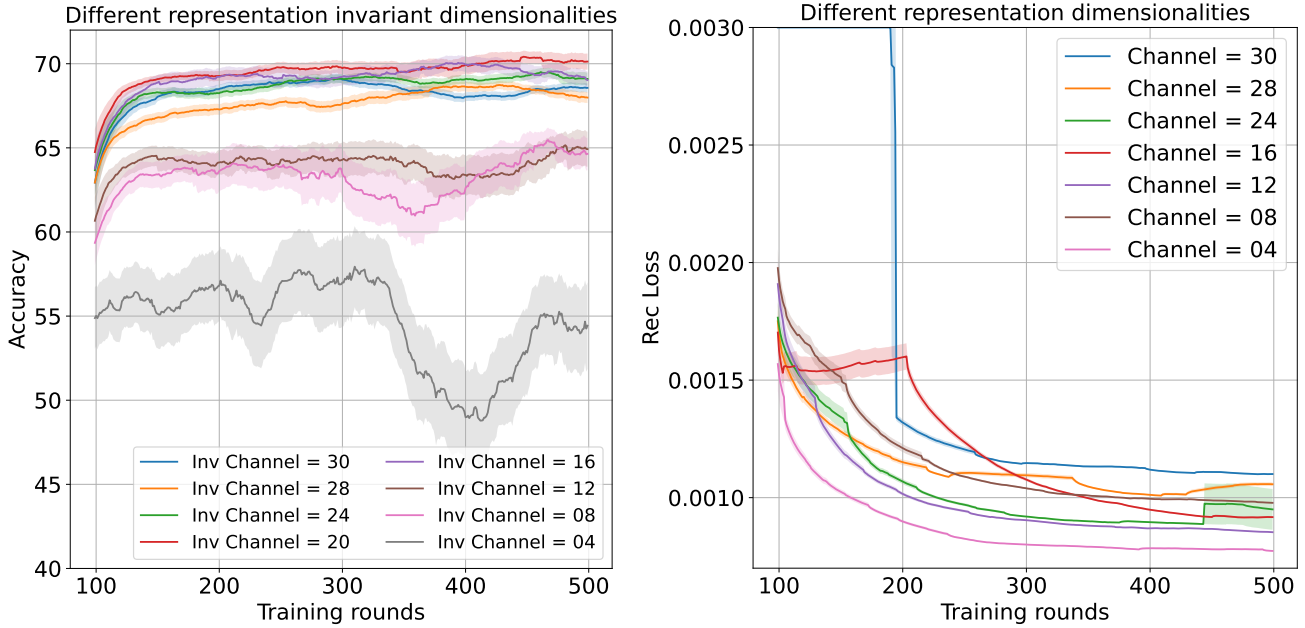


Figure 9. Illustrations of the efficacy of invariant knowledge featurizer.

I. Ablation test on unlearning stage

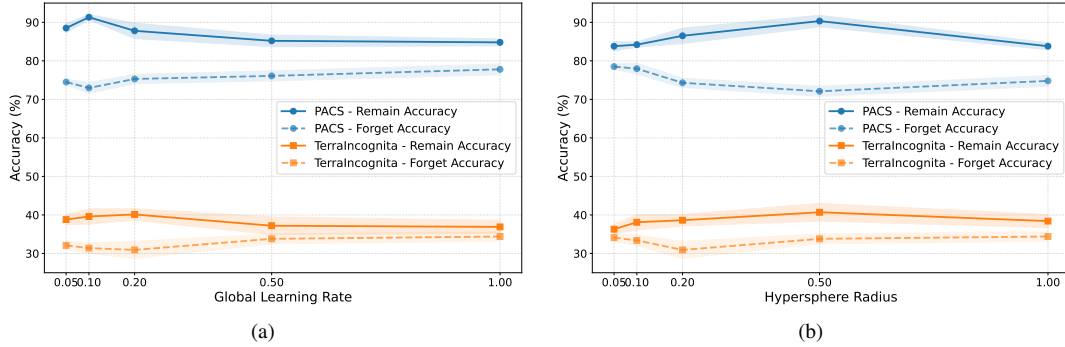


Figure 10. Effects of different global learning rates and hypersphere radii on FOUL performance. For both PACS and Terra Incognita, the model achieves the best remaining accuracy (RA) and forgetting accuracy (FA) when $\eta = 0.2$ and $\kappa = 0.5$.

Learning rate. In Fig. 10a, we present the FOUL results obtained with varying learning rates η , while fixing $\kappa = 0.5$. Each result is averaged over three independent runs. For both the PACS and TerraIncognita datasets, the gradient matching task performs best when $\eta = 0.2$, achieving the best RA and FA.

Sensitivity of gradient matching. We evaluate the sensitivity of the gradient matching process to different values of κ on two datasets. Each experiment is conducted three times, and the results are averaged. As shown in Fig. 10b, FOUL is optimal when the hypersphere radius is set to 0.5 on PACS and between 0.2 and 0.5 on TerraIncognita, where the gap between RA and FA is the largest.

Disentanglement Efficiency. To consider the disentanglement efficiency towards the unlearning phase, we deploy the ablation test according to different causal/non-causal representations dimensionality. We measure the RA and FA according to each cases and evaluate. The results is given in Figure 11.

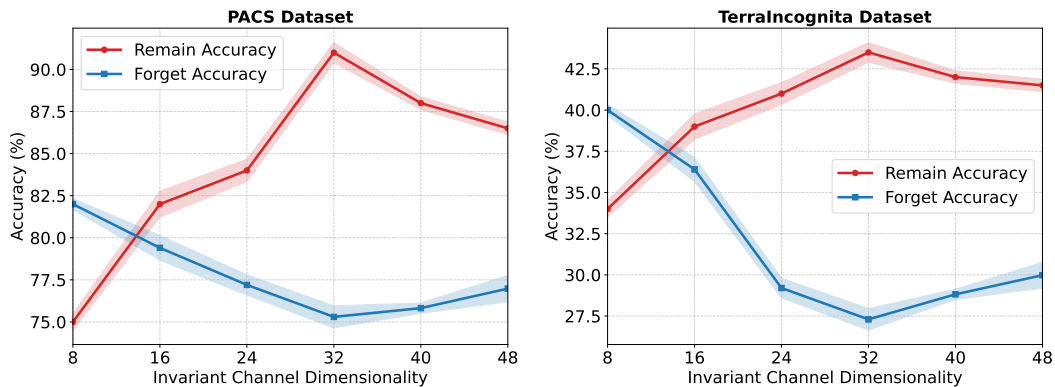


Figure 11. Ablation test on different causal dimensionality of the model disentanglement.

J. Discussion

FOUL offers an efficient unlearning mechanism by directly aggregating information from both forget and retain clients on the server. Moreover, restricting unlearning to a sub-network significantly reduces computational cost. However, FOUL also has limitations. In particular, the gradient-alignment optimization performs best when the number of clients is moderate (e.g., fewer than 100). When the client population becomes extremely large, the optimization may converge to suboptimal solutions. Addressing scalability and robustness in such large-client regimes is an important direction for future research.